



## GROWTH, SPECTRAL, NLO AND IMPEDANCE STUDIES OF POTASSIUM AMMONIUM SULPHATE CRYSTALS GROWN BY AQUEOUS SOLUTION TECHNIQUE

N. Rathna\*, V. S. John\*\*, T. Chithambarathanu\* & P. Selvarajan\*\*\*

\* Physics Research Centre, S.T Hindu College, Nagercoil, Tamilnadu

\*\* Department of Physics, T.D.M.N.S College, T. Kallikulam, Tamilnadu

\*\*\* Department of Physics, Aditanar College of Arts and Science, Tiruchendur, Tamilnadu

**Cite This Article:** N. Rathna, V. S. John, T. Chithambarathanu & P. Selvarajan, "Growth, Spectral, NLO and Impedance Studies of Potassium Ammonium Sulphate Crystals Grown by Aqueous Solution Technique", *International Journal of Applied and Advanced Scientific Research*, Volume 2, Issue 2, Page Number 304-311, 2017.

### Abstract:

Single crystals of Potassium Ammonium Sulphate (PAS) have been grown by the free evaporation method and characterized structurally, electrically, optically and mechanically. X-ray diffraction analysis indicates the crystal system as orthorhombic. The functional groups have been identified using Fourier transform infrared spectral analysis. UV-visible transmittance spectra showed wide transparency window in visible and near IR region. The hardness values of the grown sample have been found by Vickers microhardness test. Studies of electrical properties of PAS crystal using a complex impedance spectroscopy (CIS) technique show the decrease of bulk resistance with rise in temperature indicating a typical negative temperature coefficient of resistance (NTCR) type behavior similar to that of an insulator. The nature of Nyquist plots reveals the presence of bulk and grain boundary effects in PAS crystal. Moreover, the variation in dc conductivity is found to increase with temperature.

**Key Words:** Crystal Growth, Single Crystal, XRD, FTIR, Microhardness, Impedance, Relaxation Frequency & Nyquist Plot.

### 1. Introduction:

Nonlinear optical (NLO) crystals have a lot of applications in the modern areas like optical communication, optical computing and laser technology and they are classified into organic, inorganic and semiorganic NLO crystals. Organic NLO crystals are constructed by weak Van der Waals and hydrogen bonds with conjugated  $\pi$ -electrons and hence they are soft with low thermal and mechanical stability. But inorganic and semiorganic NLO crystals comparatively have higher mechanical strength and chemical stability [1-4]. Mixed NLO crystals like lithium ammonium sulfate, sodium ammonium sulfate, potassium ammonium sulfate etc can be prepared and these crystals belong to the category of inorganic NLO crystals. By literature survey it is known that lithium ammonium sulfate crystals have been mainly associated with unusual ferroelectric and ferroelastic properties [5, 6]. ESR study of mixed crystals of potassium ammonium sulfate was carried out by Abe *et al.* [7]. It is known that many works have not been done and reported on the growth and characterization of mixed crystals of potassium ammonium sulfate (PAS). In an attempt to grow the crystalline materials for industrial applications, the crystals of PAS were formed using potassium sulfate and ammonium sulfate as the reactants. Here, the aim of the paper is to report the details on crystal growth, spectral, NLO, mechanical and impedance studies of potassium ammonium sulfate crystals.

### 2. Crystal Growth:

An aqueous saturated solution was prepared by dissolving analytical grade chemicals of potassium sulfate and ammonium sulfate in 0.3:0.7 molar ratio with continuous stirring using a magnetic stirrer for five hours at room temperature. The prepared solution was filtered and kept undisturbed in a constant temperature bath maintained at a temperature of 30°C. The slow evaporation method was adopted to grow the crystals. When evaporation takes place slowly, super saturation is activated. As a result, transparent and colourless single crystals of potassium ammonium sulphate (PAS) were formed at room temperature in a period of about 15 days. The photograph of the harvested crystals of PAS is shown in the figure 1.

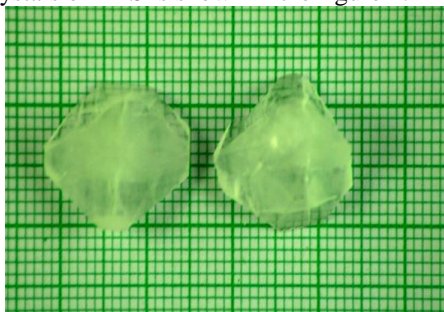


Figure 1: The grown potassium ammonium sulfate (PAS) crystal

### 3. Results and Discussion:

#### 3.1 Determination of Crystal Structure:

Single crystal X-ray diffraction analysis was carried out to determine the lattice parameters of PAS crystal. The lattice parameters and hence the structure were obtained for the sample using a ENRAF NONIUS CAD4 single crystal X-ray diffractometer with MoK<sub>α</sub> radiation ( $\lambda = 0.71069 \text{ \AA}$ ). From the single crystal XRD analysis, the data were obtained and they are presented in the table 1. From the data is observed that the grown crystals crystallize in the orthorhombic system with the space group of Pmcn. The density of the crystal is found to be 2.497 g/cc. The number of molecular units per unit cell is found to be 4 and the space group for PAS crystal is Pmcn.

Table 1: Single crystal XRD data for PAS crystal

Unit cell dimensions	a = 5.792 (2) $\text{\AA}$ , $\alpha = 90^\circ$ b = 10.147(3) $\text{\AA}$ , $\beta = 90^\circ$ c = 7.507 (5) $\text{\AA}$ , $\gamma = 90^\circ$
Volume of the unit cell	441.19(2) $\text{\AA}^3$
Z	4
Density	2.561 g/cc
Crystal system,	Orthorhombic
Space group	Pmcn

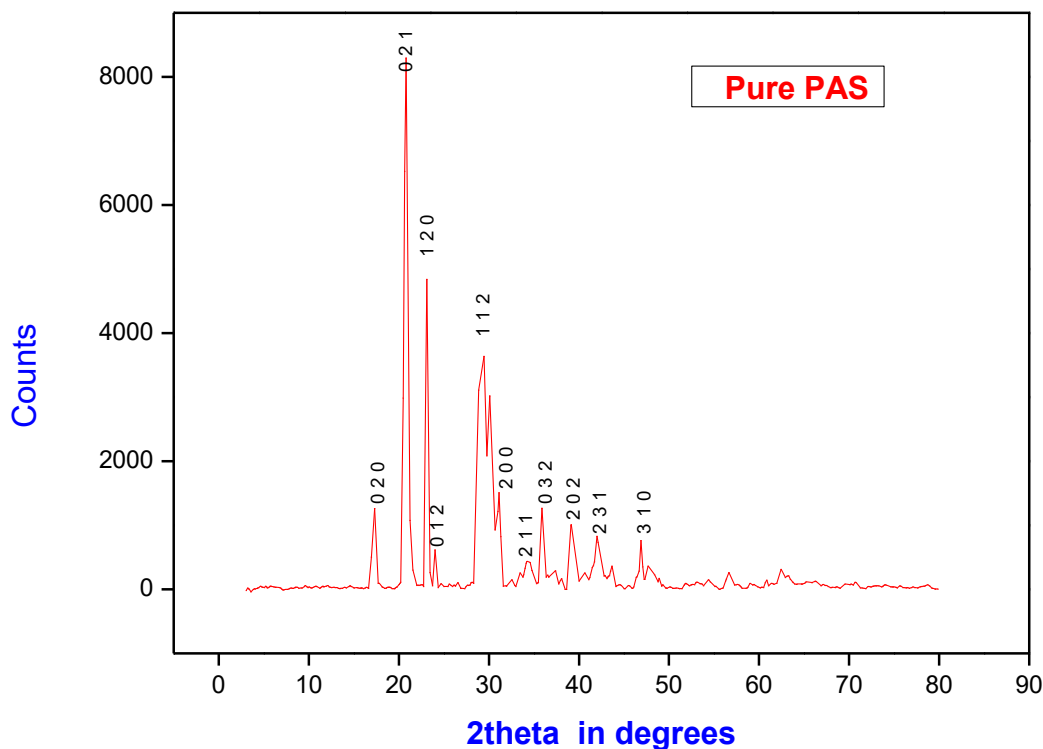


Figure 2: Powder XRD pattern of the grown PAS crystal

For the confirmation of the crystal structure obtained by single crystal XRD studies, powder X-ray diffraction studies were also carried out using a powder X-ray diffractometer in reflection scan mode. The powder XRD pattern of the grown crystal is shown in Fig. 2. The well defined Bragg's peaks at specific 2-theta angles show the high crystallinity of the sample. The diffraction peaks were indexed using the INDEXING software. The powder X-ray diffraction (XRD) pattern obtained is a well resolved one and could be fitted to an orthorhombic unit cell. The obtained powder XRD data are provided in the table 2. Using the UNITCELL software package, the unit cell parameters were evaluated from the powder XRD data and the unit cell dimensions thus obtained are a=5.7713  $\text{\AA}$  , b=10.0394  $\text{\AA}$  , c=7.5048  $\text{\AA}$  . The obtained values of unit cell parameters of PAS crystal from single crystal XRD and powder XRD methods are observed to be in good agreement with the available literature [8,9].

Table 2: Powder XRD data for PAS crystal

S.No	Angle (2θ°)	d-value (Å)	Relative Intensity (%)	h k l
1	17.721	5.0011	18	0 2 0
2	21.240	4.1797	100	0 2 1
3	23.458	3.7893	59	1 2 0
4	25.005	3.5583	10	0 1 2
5	29.472	3.0282	45	1 1 2
6	30.996	2.8828	21	2 0 0
7	34.211	2.6189	8	2 1 1
8	35.888	2.5002	18	0 3 2
9	39.146	2.2993	15	2 0 2
10	42.891	2.1068	12	2 3 1
11	47.699	1.9050	13	3 1 0

### 3.2 Optical Transmittance Studies:

Transmission spectra are very important for any NLO materials, because a nonlinear optical material can be of any practical use if it has a wide transparency window. In the present study, we have recorded the UV-Vis-NIR transmission spectrum in the range of 190 nm-1100 nm and is shown in Fig. 3. The instrument used in the analysis is LAMBDA-35 UV-Vis spectrophotometer. The crystals are transparent in the visible and infrared spectral regions. It can be seen from the transmission curve that the lower cutoff wavelength is obtained at 282 nm. The material is found to be transparent to all radiations in the wavelength range 300 nm-1100 nm. The absence of absorption in the visible region clearly indicates that PAS crystal can be used as window material in optical instruments [8]. Using the formula  $E_g = 1242 / \lambda$  (nm), the band gap is calculated to be 4.405 eV. The peak near the fundamental absorption indicates that this crystal is an indirect band gap material.

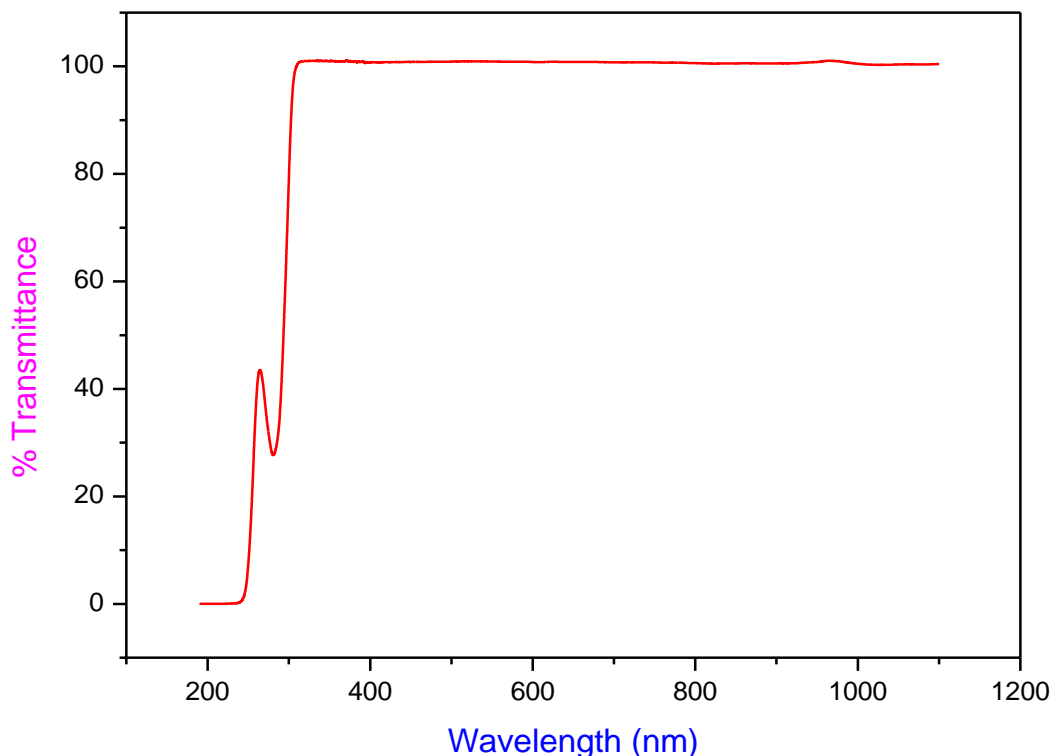


Figure 3: UV-Vis-NIR transmittance spectrum of PAS crystal

### 3.3 FTIR Spectral Analysis:

Fourier transform infrared (FTIR) spectrum was recorded by the KBr pellet method for the grown PAS crystal in the wave number of 400-4000  $\text{cm}^{-1}$  by using a SHIMADZU spectrometer. The FTIR spectra of PAS crystal is shown in the Fig.4. The absorption peaks observed at 3122.98  $\text{cm}^{-1}$  are attributed to  $\text{NH}_4^+$  groups. Multiple combination and overtone bands extend the absorption to about 2080.66  $\text{cm}^{-1}$ . The absorption at 1337  $\text{cm}^{-1}$  is due to bending vibrations of  $\text{NH}_4^+$  groups. Observation of peaks at nearly 1111.49 and 620.68  $\text{cm}^{-1}$  can

be assigned to the  $\text{SO}_4^{2-}$  vibrations. The presence of various functional groups of the grown crystal is in good agreement with those reported in the literature [9].

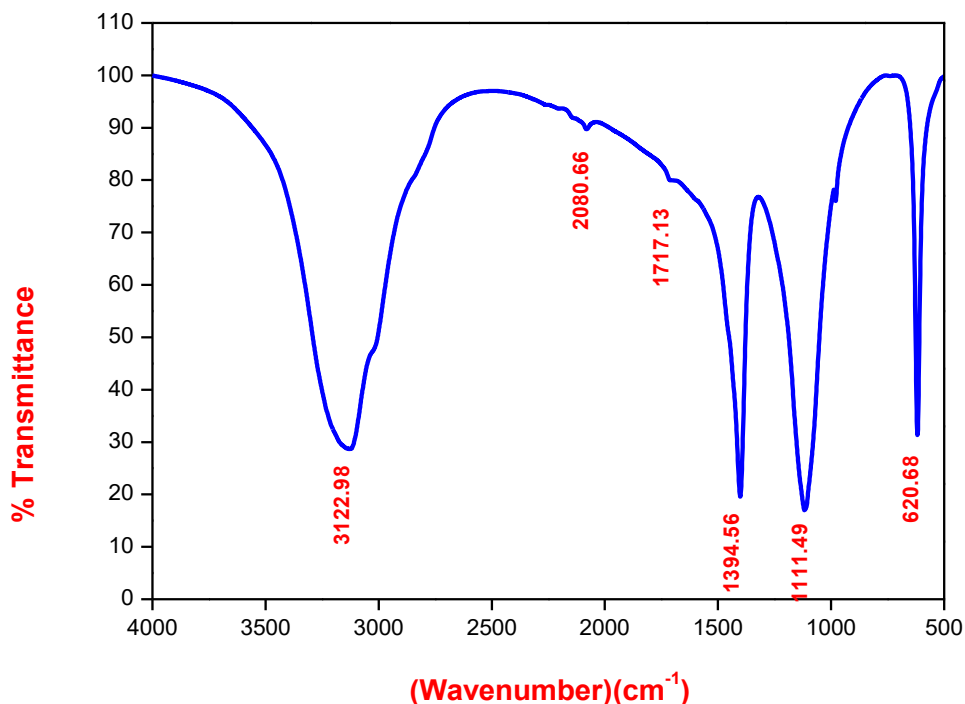


Figure 4: FTIR spectrum of PAS crystal

Table 2: Observed FTIR vibrational assignments for PAS crystal

Wave Number (cm <sup>-1</sup> )	Assignments
3122.98	NH <sub>4</sub> <sup>+</sup> stretching
1394.56	NH <sub>4</sub> <sup>+</sup> bending
1111.49	SO <sub>4</sub> <sup>2-</sup> stretching
620.68	SO <sub>4</sub> <sup>2-</sup> bending

### 3.4 Hardness Test:

Hardness is a measure of the resistance to plastic deformation. The hardness of the crystal carries information about the strength, molecular bindings, yield strength and elastic constants of the material. The hardness tests for PAS crystal was carried out by a micro hardness tester fitted with a Vickers diamond pyramidal indenter. The diagonal length of the indentation for various applied loads in gm is measured for a constant indentation period of 10 sec. The hardness values were calculated from the formula  $H_v = 1.8544 P/d^2$  where P is the applied load in kg, d is mean diagonal length of the indentation in mm [10]. Graph (Fig.5) shows that the hardness increases with the increase of load due to the release of internal stress generated by indentation. The phenomenon of dependence of microhardness of a solid on the applied load, at low level of testing load is known as indentation size effect. Meyer's law [11] relates load and size of the indentation as  $Pd^n$  where a and n are constants for a given material. The work hardening coefficient was found to be 3.0232 by taking a slope in the straight line of the graph (Fig. 6) drawn between log P and log d. According to Onitsch and Hanneman 'n' should lie between 1 and 1.6 for hard materials and is greater than 1.6 for soft materials [12]. The 'n' value observed in the present studies is around 3.02341 suggests that the grown PAS crystal belongs to soft material category.

From the hardness number, the yield strength ( $\sigma_y$ ) has been calculated using the relation (for  $n > 2$ )  $\sigma_y = (H_v \times (0.1)^{n-2}) / 3$ . The calculated values of yield strength  $\sigma_y$  for PAS crystal is shown in the Table 3. The elastic stiffness constant ( $C_{11}$ ) has been calculated for the grown crystal using Wooster's empirical relation  $C_{11} = H_v^{7/4}$  [13,14]. The calculated stiffness constant and yield strength for different loads are given in the Table 3. It is observed from the results that the hardness, yield strength and stiffness constant increase with increase of the applied load and this crystal has the reverse indentation size effect.

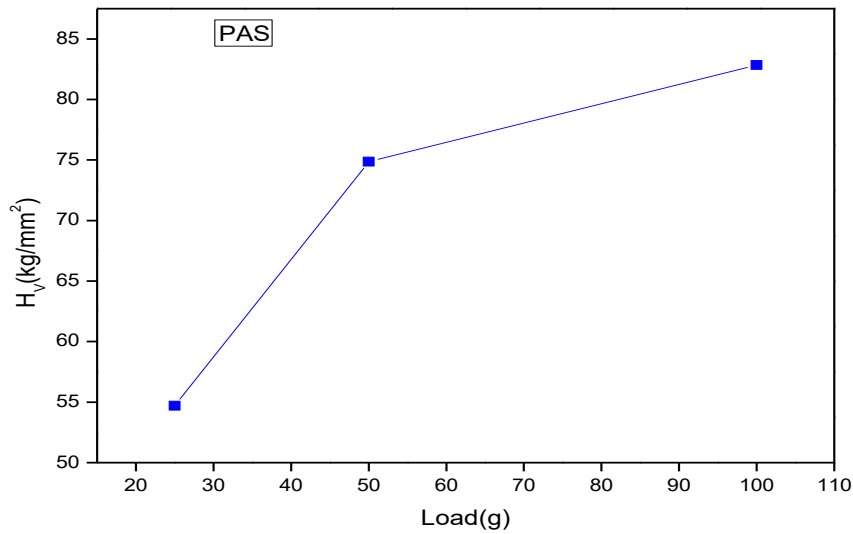


Figure 5: Variation of microhardness number with the applied load for PAS crystal

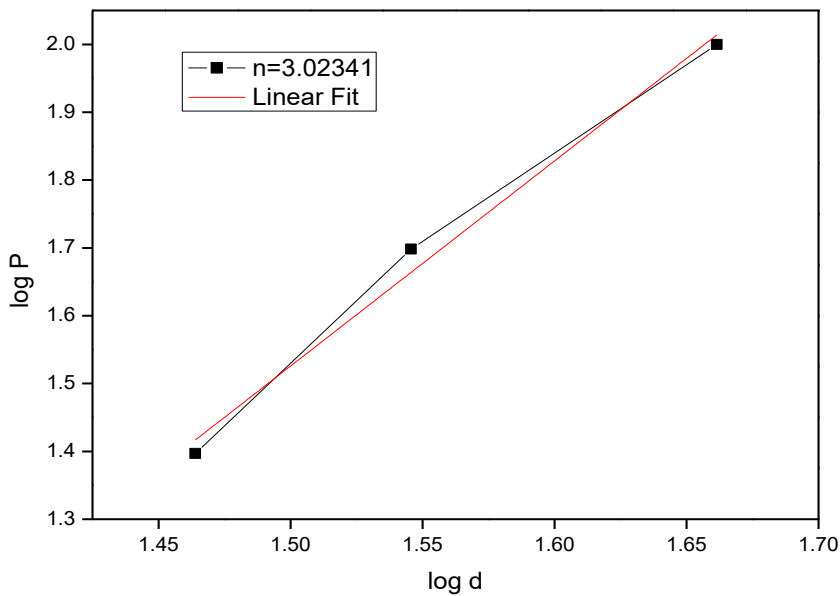


Figure 6: Plot of Log P versus Log d for PAS crystal

Table 3: Yield Strength and Stiffness constant for PAS crystal

Grown crystal	Load (g)	Vicker hardness Number $H_v$ (kg/mm <sup>2</sup> )	Yield strength $\sigma_y$ (M Pa)	Stiffness Constant $C_{11} \times 10^{14}$ (Pa)
PAS	25	54.7	16.9309	18.8852
	50	74.85	23.1678	32.6949
	100	82.85	25.6440	39.0532

### 3.5 Impedance Analysis:

Impedance spectroscopy is a powerful technique for the characterization of electrical behaviour of NLO materials and defined as the frequency domain ratio of the voltage to the current and it is the opposition of the flow of alternating current (AC) in a complex system [15, 16]. The frequency dependent properties of a material are often represented as complex impedance  $Z^*$  and which is related as  $Z^*(\omega) = Z' - jZ''$  where  $Z'$  and  $Z''$  are the real and imaginary components of impedance. The variations of real part of impedance ( $Z'$ ) and imaginary part of impedance ( $Z''$ ) with frequencies at temperatures are shown in the Figs.7 and 8. From the result it is observed that the real and imaginary part of impedance decreases with the increase in temperature and

frequency. This decrease of impedance gives an indication of negative temperature coefficient of resistance behavior like that of an insulator. The high value of impedance at low frequency indicates low ionic mobility in the grown PAS crystal. The peaks in the plots of impedance versus frequency are corresponding to relaxation process and the peak frequency is equal to relaxation frequency. The Nyquist plots for the grown PAS crystal have been drawn between real part and imaginary part of impedance at different temperatures and they are presented in Fig.9. These plots show semicircles which indicate the transport response function characteristically, one semicircular arcs and spikes and these plots reveal the presence of bulk effect and grain boundary effect of the sample. Semicircles at low frequencies are considered due to the grain boundary where as the semicircles at higher frequencies depict the bulk effect. The bulk effect arises due to the parallel combination of bulk resistance and bulk capacitance of the sample [17, 18].

DC conductivity values for the grown PAS was calculated using the following formula

$$\sigma_{dc} = d/AR_b \text{ (ohm m)}^{-1}$$

Where  $\sigma_{dc}$  is the DC conductivity,  $d$  is the thickness of the sample and  $A$  is the area of the faces in contact with the electrodes and  $R_b$  is the bulk resistance values obtained from the Nyquist plots. Table 4 shows the DC conductivity values of grown PAS crystal. It is observed from the results that DC conductivity increases with increase of temperature, which is associated with the decrease in bulk resistance. The alteration in the values of complex impedance, bulk resistance, grain boundary resistance and DC conductivity of the grown samples may be due to the polarizing nature of the samples and changes in mobility of the charge carriers by size of ions and it brings prominent changes in the electronic band structure.

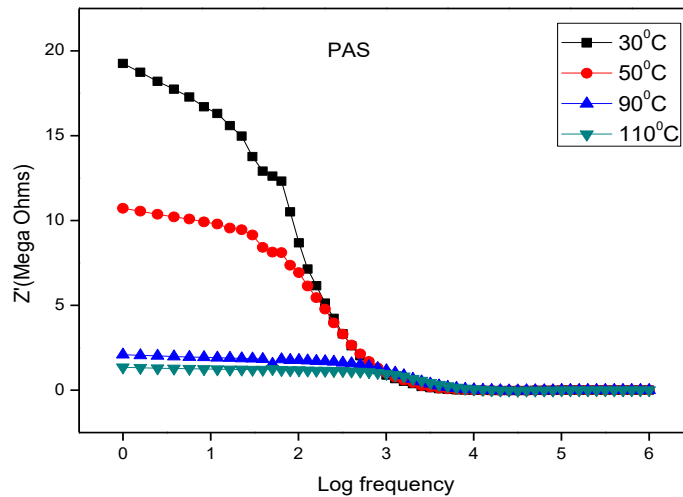


Figure 7: Frequency dependence of real part of impedance for PAS crystal at different temperatures

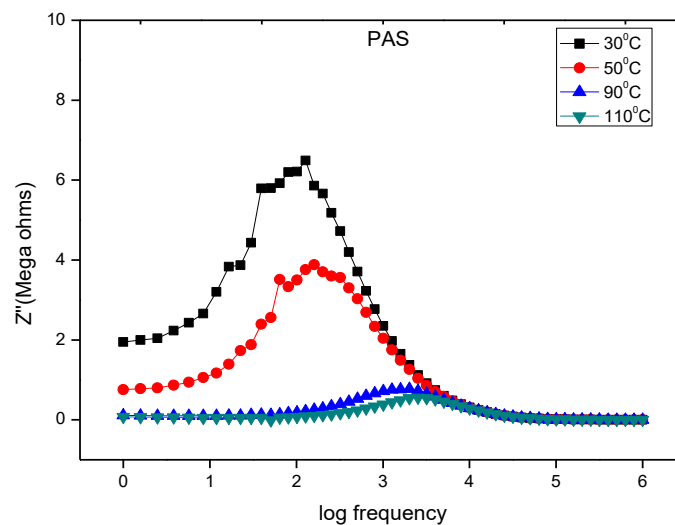


Figure 8: Frequency dependence of imaginary part of impedance for PAS crystal at different temperatures

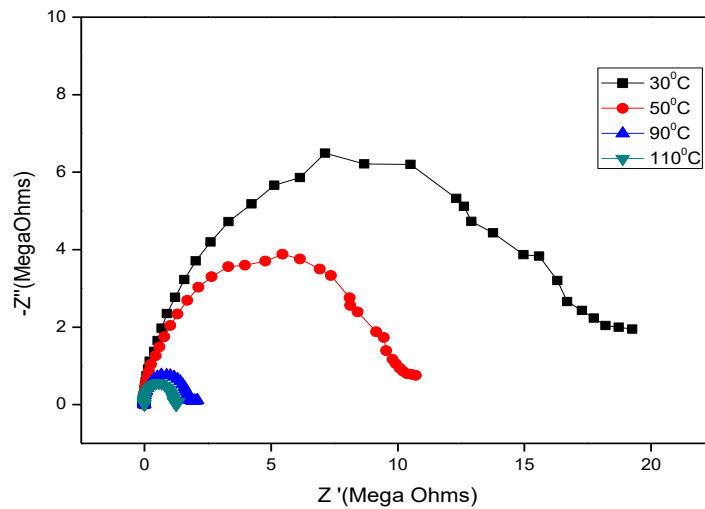


Figure 9: Nyquist plots for PAS crystal at (i) 30 °C, (ii) at 50 °C, (iii) at 90 °C and (iv) at 110 °C

Table 4: The values of bulk resistance, grain boundary resistance and DC conductivity values of the grown PAS crystal

S.No.	Sample	Temperature (°C)	Bulk Resistance $R_b$ (ohm)	Grain boundary resistance $R_{gb}$ (ohm)	DC conductivity $(\Omega m)^{-1}$
1	PAS	30	$19.27 \times 10^6$	$9.62 \times 10^6$	$8.59 \times 10^{-7}$
		50	$10.67 \times 10^6$	$5.31 \times 10^6$	$15.52 \times 10^{-7}$
		90	$2.08 \times 10^6$	$0.97 \times 10^6$	$79.617 \times 10^{-7}$
		110	$1.31 \times 10^6$	$0.59 \times 10^6$	$126.41 \times 10^{-7}$

### 3.6 Relaxation Frequency and Relaxation Time:

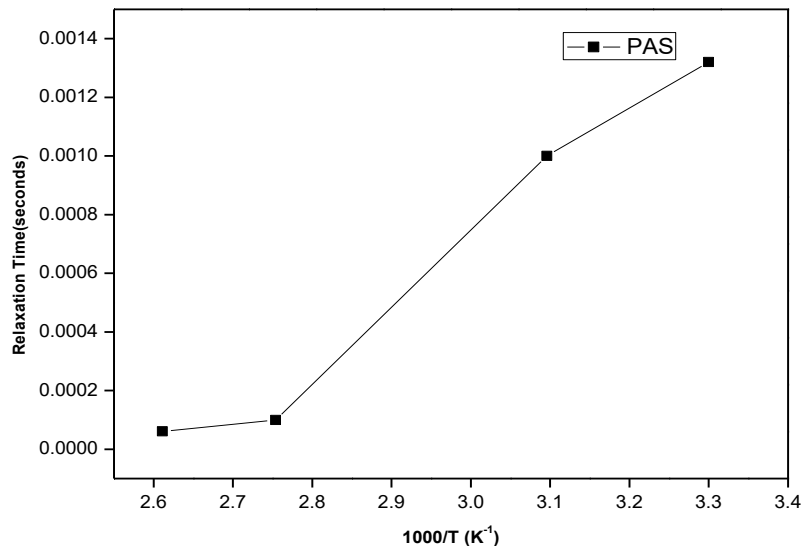


Figure 10: Variation of relaxation time with temperature for PAS crystal

Relaxation frequency and relaxation time were obtained using the values of impedance data. Each semicircular arc in the Nyquist plot has its own characteristic features having a unique relaxation frequency ( $\omega_{max}$ ) attributed to electrical phenomena in the sample. Relaxation frequency can be expressed as  $\omega_{max} = 1/\tau$  where  $\tau$  is the relaxation time and it depends on the intrinsic property of material. The values of relaxation frequency are obtained from imaginary plots of impedance and also from Nyquist plots. The relaxation process may be due to the presence of immobile species at low temperatures and defects at higher temperatures. The shifting of relaxation frequency to the higher side in imaginary impedance plots with increasing temperature indicates the increasing energy loss in the sample. The relaxation time ( $\tau$ ) is calculated using the value of

relaxation frequency. Fig.10 shows the variation of relaxation time ( $\tau$ ) as a function of inverse of absolute temperature and the relaxation time of the sample is observed to be decreasing with increase of temperature of the sample. Hence, it is concluded that relaxation time of the grown sample is temperature dependent.

#### **4. Conclusion:**

Transparent good quality single crystals of potassium ammonium sulphate were grown by slow evaporation technique from a mixture of aqueous solutions of potassium Sulphate and ammonium sulphate at constant temperature of 30°C. The lattice parameters were found by single crystal XRD and powder XRD methods. The FTIR spectrum was recorded for the sample and functional groups were identified. Optical transmittance spectrum confirms that the grown crystal of PAS is suitable for NLO applications because it has high transparency and high optical band gap. Microhardness study of the sample has been carried out to understand the behaviour of mechanical strength of the sample. The electrical parameters such as the real part of impedance ( $Z'$ ), the imaginary part of impedance ( $Z''$ ) and DC conductivity as a function of both frequency and temperature have been studied through impedance spectroscopy. Nyquists plot reveals that both bulk and grain boundary resistance decreases with rise in temperature. The electrical relaxation process occurring in the material has been found to be temperature dependent and an increase in dc conductivity of the sample with increase in temperature is also observed.

#### **5. Acknowledgement:**

The authors would like to thank the staff members of Cochin University (Cochin), PSN college of Engineering (Tirunelveli), St. Joseph's college (Trichy) for helping to take the research data.

#### **6. References:**

1. N. Bloembergen, *J Nonlinear OPT. Phys. Mater* 15(1996)1.
2. Badan. J, Hierle. R, Perigaud. A, Zyss. J, *Nonlinear optical properties of organic molecules and Polymeric materials*. 3<sup>rd</sup> ed. Washington: DC; 1993.
3. Y. R. Shen, *The Principles of Nonlinear Optics*, Wiley, New York, 1984.
4. H. O. Marcy, L. F. Warren, M. S. Webb, C. A. Ebberts, S. P. Velsko, G. C. Kennedy, *Appl. Opt*, 31, 5051 (1992).
5. W. A. Dollase, *Acta Crystallogr. B* 25 (1969)2298.
6. K. Itoh, H. Ishikur and E. Nakamura, *Acta Crystallogr. B* 37 (1981)664.
7. R. Abe, N. Shibata and K. Dejima, *Ferroelectrics* 20(1978) 217-218.
8. S. Ledoux, J. Zyss, *J. Int. Nonlinear Opt. Phys.*, 3, 287(1994)
9. A. Karolin, K. Jeyakumari, C. K. Mahadevan *IJ. Engg Res. and App.* Vol.3, (2013) 1906- 1915.
10. B. Sivasankari and P. Selvarajan, *J. Experimental Sciences* 1(2010), 31.
11. E. Meyer, *Z. Verein, Duet. Ing.* 52(1908), 645.
12. E. M. Onitsch, *Mikroskopie*, 95 (1956)12.
13. Wooster W A, *Rep. Progr. Phys.*, 16 (1953) 62.
14. Ezhil Vizhi R, Rajan Babu D & Sahyanarayanan K, *Ferroelectrics Lett. Sec.*, 37(2) (2010) 23.
15. Banarji Behera, P. Nayak, R.N.P. Choudhary, *Mater. Res. Bull.* 43 (2008) 401.
16. V. C. Veeranna Gowda, R.V. Anavekar, *Solid State Ionics* 176 (2005) 1393.
17. B. Behera, P. Nayak, R.N.P. Choudhary, *J. Alloys Compd.* 436 (2007) 226.
18. P. B. Macedo, C.T. Moynihan, R. Bose, *Phys. Chem. Glasses* 13 (1972) 171.